Published in final edited form as:
Inorganica Chim Acta. 2010 October 15; 363(12): 2728–2733. doi:10.1016/j.ica.2010.05.006.

Nickel(II) complexes stabilized by bis[N-(6-pivalamido-2-pyridylmethyl)]benzylamine: Synthesis and characterization of complexes stabilized by a hydrogen bonding network

Darla A. Powell-Jia, **Melinda T.-N. Pham**, **Joseph W. Ziller**, and **A. S. Borovik**
Department of Chemistry, University of California Irvine, 1102 Natural Science II, Irvine, CA 92697 USA

Abstract

Hydrogen bonds in metalloproteins are key in directing reactivity yet to be achieved in synthetic systems. We have been developing a synthetic system that uses hydrogen-bonding interactions to modulate the secondary coordination around a transition metal ion. This was accomplished with the ligand bis[*N*-(6-pivalamido-2-pyridylmethyl)]benzylamine (H_2pmb), which contains two carboxyamido units appended from pyridine rings. Several nickel complexes were prepared and structurally characterized. In particular, we found that the appended carboxyamido groups either provide intramolecular H-bond donors or can be converted to bind directly to a metal center. We established that the complex $Ni^{II}H_2pmb(Cl)_2$ can be sequentially deprotonated with potassium *tert*-butoxide, causing coordination of the carboxyamido oxygen atoms and concomitant loss of the chloro ligands. The chloro ligands were also removed with silver(I) salts—in the presence of acetate ions, the complex $Ni^{II}H_2pmb(\kappa^2\text{-OAc})(\kappa^1\text{-OAc})$ was isolated, in which an intramolecular H-bonding network occurs between the H_2pmb ligand and the coordinate acetato ligands.

1. Introduction

Hydrogen bonds (H-bonds) within the secondary coordination sphere are important in controlling the structure and function of metal complexes.[i] This is typified within the active sites of metalloproteins, wherein protein-derived H-bonding networks affect a variety of structural and physical properties that are ultimately correlated to activity.[ii] These findings have inspired the development of synthetic systems that attempt to create similar H-bonding networks within the secondary coordination sphere of transition metal complexes.[iii] The most common designs utilize multidentate ligands that contain a metal ion-binding pocket and appended functional groups that can position H-bond donors/acceptors proximal to bound metal ions. In addition, most of these ligands form relatively rigid cavities in order to promote formation of *intramolecular* H-bonds. Several systems have featured the carboxyamidopyridyl moiety, which has been successful in forming intramolecular H-bonds to other coordinated species (Fig. 1A). First introduced by Masuda within a symmetrical tripodal ligand,[iv] several derivatives now exist that are being used to probe H-bonding effects.[v,vi]

Supplementary Information.
CIF format for X-ray analyses of $Ni^{II}H_2pmb(Cl)_2$, $Ni^{II}Hpmb(Cl)$, $Ni^{II}pmb(THF)$, and $Ni^{II}H_2pmb(\kappa^2\text{-OAc})(\kappa^1\text{-OAc})\cdot CH_3CN$.

In the structure depicted in Fig. 1A, the pyridyl groups coordinate to the metal center and the carboxyamido portion serves as the H-bond donor to another ligand. However, another binding mode for the carboxyamidopyridyl moiety is also possible, in which the pyridyl nitrogen and the carbonyl oxygen atoms both bind to a metal ion (Fig. 1B).[5,6,vii] This bidentate chelation could be a convenient means for controlling access to a metal ion and modulating the properties of metal complexes. Toward these goals we have been exploring the Ni(II) coordination chemistry with the ligand bis(*N*-pivalamido-2-pyridylmethyl)benzylamine (H_2pmb) that contains two carboxyamidopyridyl units (Fig. 1C). This report describes the syntheses, molecular structures, and physical properties for a series of Ni(II) complexes with this ligand that illustrate the utility of incorporating carboxyamidopyridyl units into the design of metal complexes.

2. Experimental

2.1. Preparative Methods and Syntheses

All reagents were purchased from commercial sources and used as received, unless otherwise noted. Solvents were purged with argon and dried over columns containing Q-5 (supported redox catalyst for dioxygen removal) and molecular sieves. Syntheses of air-sensitive metal complexes were conducted in a Vacuum Atmospheres, Co. (Hawthorne, CA) drybox under an argon atmosphere. The H_2pmb ligand was prepared following a literature procedure.[viii] Elemental analyses for $Ni^{II}H_2$pmb and $Ni^{II}H_2$pmb(κ^2-OAc)(κ^1-OAc) consistently gave low values for the percentages of carbon and nitrogen. We thus report high-resolution mass spectral data for these complexes.

2.2. Preparation of Complexes

2.2.1. {(Bis[N-(6-pivalamido-2-pyridylmethyl)]benzylamine) (dichloro)}nickelate(II) ($Ni^{II}H_2pmbCl_2$)—A solution of H_2pmb (50 mg, 0.103 mmol) in 3 mL of methanol was treated with $NiCl_2 \cdot 6H_2O$ (25 mg, 0.052 mmol). The solution turned dark green and was stirred for 10 minutes. Orange crystals were obtained through diffusion with diethyl ether into methanol (46 mg, 72%). Found: C, 55.44; H, 6.22; N, 11.24%. $Ni^{II}H_2pmbCl_2 \cdot 1/2MeOH$ ($C_{29.5}H_{39}N_5O_{2.5}NiCl_2$) requires C, 55.95; H, 6.21: N, 11.06%. FT-IR/cm^{-1} (Nujol): ν(NH) = 3297; λ_{max} (THF, nm (ε, $M^{-1}cm^{-1}$)) 20 °C: 461 (124), −100 °C: 429 (89), λ_{max} (Acetone, nm (ε, $M^{-1}cm^{-1}$)) 20 °C: 457 (101) and −90 °C: 417 (53), λ_{max} (MeCN, nm, (ε, $M^{-1}cm^{-1}$)) 20 °C: 452 (88) and −40 °C: 446 (79), λ_{max} (DCM, nm (ε, $M^{-1}cm^{-1}$)) 20 °C: 452 (100) and −80 °C: 442 (42), λ_{max} (MeOH, nm, (ε, $M^{-1}cm^{-1}$)) 20 °C: 597 (11) and −90 °C: 555 (32); μ_{eff} = 2.86.

2.2.2. {(Bis[N-(6-pivalamido-2-pyridylmethyl)]benzylamine) (diacetato)}nickelate(II) ($Ni^{II}H_2$pmb(κ^2-OAc)(κ^1-OAc))—A solution of $Ni^{II}H_2pmbCl_2$ (58 mg, 0.081 mmol) in 3 mL of 1:1 MeCN:THF was treated with Me_4NOAc (22 mg, 1.6 mmol). The orange solution was stirred for 15 minutes, then $AgBF_4$ was added and allowed to stir for an additional 10 min then filtered over Celite to remove AgCl. The volitles were removed and the resulting blue solid was redissolved in THF. Blue crystals were obtained via pentane diffusion into THF solution (45 mg, 84%). FT-IR/cm^{-1} (Nujol): ν(NH) 3406, 3315; λ_{max} (THF, nm (ε, $M^{-1}cm^{-1}$)) 20 °C: 651 (16) and −100 °C: 639 (39), λ_{max} (MeCN, nm (ε, $M^{-1}cm^{-1}$)) 20 °C: 656 (20) and −40 °C: 645 (26), λ_{max} (Acetone, nm (ε, $M^{-1}cm^{-1}$)) 20 °C: 646 (19) and −80 °C: 645 (33); μ_{eff} = 2.84; HRMS (ES+): Exact mass calcd for $C_{31}H_{40}N_5NiO_4$ [M − OAc], 604.2433. Found 604.2408.

2.2.3. {(Bis[N-(6-pivalamido-2-pyridylmethyl)][O-carboxyamido]benzylamine]) (chloro)} nickelate(II) (Ni^{II}HpmbCl)—Under argon, a solution of $Ni^{II}H_2pmbCl_2$ (50 mg, 0.081 mmol) in 3 mL of THF was treated with $KOBu^t$ (9.1 mg, 0.081mmol) and was allowed to stir for 20 minutes. Green crystals were obtained via pentane diffusion into a THF solution (46 mg, 98%). FT-IR/cm^{-1} (Nujol): ν(NH)3264, 3180; λ_{max} (THF, nm (ε, M^{-1}cm^{-1})) 20 °C: 655 (35) and −100 °C: 639 (39). λ_{max} (DCM, nm (ε, M^{-1}cm^{-1})) 20 °C: 635 (25) and −90 °C: 635 (44); μ_{eff} = 2.88; HRMS (APCI): Exact mass calcd for $C_{29}H_{36}N_5NiO_2Cl$ [M + H], 580.1989. Found 580.1995.

2.2.4. {(Bis[N-(6-pivalamido-2-pyridylmethyl)-O-carboxyamido]benzylamine])}-nickelate(II) (Ni^{II}pmb)—Under argon, a solution of Ni^{II}H$_2$pmbCl$_2$ (25 mg, 0.041 mmol) in 3 mL of 1:1 THF:MeCN was treated with KOBu^t (9.1 mg, 0.081 mmol) and was allowed to stir for 20 min. Volatiles were removed under reduced pressure. The resulting green residue was dissolved in THF and crystals were obtained via pentane diffusion (13 mg, 59%). Found: C, 63.77; H, 7.58; N, 11.16%. Ni^{II}pmb·THF ($C_{33}H_{43}N_5O_3Ni$) requires C, 64.30; H, 7.03: N, 11.36%. FT-IR/cm^{-1} (Nujol): ν(NH) 3347; λ_{max} (THF, nm (ε, M^{-1}cm^{-1})) 20 °C: 446 (29); μ_{eff} = 2.76; HRMS (ES+): Exact mass calcd for $C_{29}H_{35}N_5NiO_2$ [M + H], 544.222. Found 544.2215.

2.3. Physical Methods

NMR spectra were obtained on either Bruker DRX-400 MHz or Bruker Advance 500 MHz spectrometers. NMR solvents were used as received. Electronic spectra were recorded with an Agilent 8453 spectrophotometer. FT-IR spectra were collected on a Varian 800 Scimitar Series FT-IR spectrophotometer and are reported in wavenumbers. Mass spectra were recorded on a Waters LCT Premier mass spectrometer operated in EI or APCI mode. Magnetic moments were determined using Evan's method in DMSO.[ix] Elemental analyses were performed on a Perkin-Elmer 2400 Series II CHNS analyzer.

2.4.1. Crystallographic Structural Determination—Intensity data for the complexes were collected using a Bruker SMART APEX II diffractometer using graphite-monochromated Mo Kα radiation (λ=0.71073 Å). The SMART[x] program package was used to determine the unit-cell parameters and for data collection (25 s/frame scan time) for a sphere of diffraction data. The raw frame data was processed using SAINT[xi] and SADABS[xii] to yield the reflection data files. Subsequent calculations were carried out using the SHELXTL[xiii] program. The structure was solved by direct methods and refined on F^2 by full-matrix least-squares techniques. The analytical scattering factors[xiv] for neutral atoms were used throughout the analysis.

2.4.1.1. Ni^{II}H$_2$pmbCl$_2$: A green crystal of approximate dimensions 0.15 × 0.21 × 0.23 mm was used, giving diffraction symmetry of 2/m and systematic absences consistent with the monoclinic space group P2$_1$/c. The structure was solved by direct methods and refined on F^2 by full-matrix least-squares techniques. Hydrogen atoms associated with atoms C(20), C(21), and C(22) were included using a riding model.

2.4.1.2 Ni^{II}H$_2$pmb(κ^2-OAc)(κ^1-OAc)·CH$_3$CN: A blue crystal of approximate dimensions 0.07 × 0.26 × 0.27 mm was employed, giving diffraction symmetry of 2/*m* and the systematic absences consistent with the monoclinic space groups *P*2/ and *Pc*. It was later determined that space group *Pc* was correct. Hydrogen atoms were either located from a difference-Fourier map and refined (x,y,z and Uiso) or were included using a riding model. There were two molecules of the formula-unit and two molecules of acetonitrile solvent present. Attempts to solve the structure in space group *P*2/*c* were unsuccessful. Analysis of the data using the PLATON[xv] program package suggested the space group assignment was correct. The structure was refined using the TWIN instruction[xvi], BASF = 0.372.

2.4.1.3. Ni^{II}HpmbCl: A gold-green crystal of approximate dimensions 0.15 × 0.30 × 0.35 mm gave diffraction symmetry of 2/m and the systematic absences consistent with the monoclinic space group $P2_1/n$ that was later determined to be correct. Hydrogen atoms were included using a riding model. There were two molecules of the formula-unit present (Z = 8).

2.4.1.4. Ni^{II}pmb(THF): The crystal of this complex isolated contained one coordinated THF molecule. A colorless crystal of approximate dimensions 0.13 × 0.13 × 0.22 mm was mounted on a glass fiber and transferred to the diffractometer. There were no systematic absences or any diffraction symmetry other than the Friedel condition. The centrosymmetric triclinic space group $P\bar{1}$ was assigned and later determined to be correct. Hydrogen atoms were included using a riding model. Carbon atoms C(9), C(10), C(11), C(30), C(31), C(32) and C(33) were disordered and included using multiple components, partial site-occupancy-factors and isotropic thermal parameters. At convergence, wR2 = 0.1032 and Goof = 1.028 for 381 variables refined against 6753 data (0.78Å), R1 = 0.0399 for those 5622 data with $I > 2.0\sigma(I)$.

3. Results and discussion

3.1. Synthesis and Solution Studies

The ligand H$_2$pmb is similar to other dipyridylamine ligands used in coordination chemistry.[xvii] The key difference is the appended carboxyamido groups that can affect both the primary and secondary coordination spheres. To explore this premise we have prepared a series of Ni(II) complexes, starting with the parent complex, Ni^{II}H$_2$ pmb(Cl$_2$) (Scheme 1). This complex was readily prepared by treating a methanolic solution of H$_2$pmb with Ni^{II}Cl$_2$. The complex was isolated via vapor diffusion of diethyl ether to afford orange crystals in a 72% yield.

The appended carboxyamido groups in Ni^{II}H$_2$pmb(Cl)$_2$ could be deprotonated under basic conditions, causing loss of the chloro ligands with concomitant amidate coordination to the nickel center (Scheme 2). For example, the monochloro complex, Ni^{II}Hpmb(Cl) was produced in nearly quantitative yield when Ni^{II}H$_2$ pmb(Cl$_2$) was allowed to react with 1 equiv of KOBu^t in THF.

In addition, Ni^{II}pmb was isolated (59% yield) when 2 equiv of KOBu^t were reacted with Ni^{II}H$_2$pmb(Cl)$_2$. Note too that Ni^{II}pmb was prepared from NiHpmbCl and 1 equiv of the base. Removal of the chloro ligands was also achieved using AgBF$_4$ in the presence of acetate. In this case, two acetate ions coordinate to the nickel center, affording the complex Ni^{II}H$_2$pmb(κ^2-OAc) (κ^1-OAc) in a yield of 84%.

All the Ni^{II} complexes are paramagnetic at room temperature with solution effective magnetic moments between 2.8–2.9 μ_{BM}. These values are near the spin-only value of 2.83 μ_{BM} expected for an $S = 1$ spin system.[xviii] The chloro complexes and Ni^{II}H$_2$pmb(κ^2-OAc) (κ^1-OAc) have temperature-dependent optical properties, in which a red-shift in the absorbance bands occurred with decreased temperature. For instance, the 20°C absorbance spectrum of Ni^{II}H$_2$ pmb(Cl)$_2$ in acetone has a peak at λ_{max} = 452 nm that shifts to at λ_{max} = 442 nm at −80°C.

3.2. Molecular Structures

The molecular structures of the nickel complexes were examined in the solid-state using X-ray diffraction methods. Thermal ellipsoid diagrams of Ni^{II}H$_2$pmb(Cl)$_2$ and Ni^{II}Hpmb(Cl) are found in Fig. 2, and Ni^{II}pmb(THF) and Ni^{II}H$_2$pmb(κ^2-OAc)(κ^1-OAc) are shown in Fig.

3. Crystal, data collection, and refinement parameters are found in Table 1. Selected angles and distances are given in Tables 2 and 3.

3.2.1. Molecular Structures of $Ni^{II}H_2pmb(Cl)_2$ and $Ni^{II}Hpmb(Cl)$—

The complexes $Ni^{II}H_2pmb(Cl)_2$ and $Ni^{II}Hpmb(Cl)$ crystallized in the monoclinic space groups $P2_1/c$ and $P2_1/n$, respectively. The asymmetric unit for $Ni^{II}Hpmb(Cl)$ contained two crystallographically independent, but chemically identical, molecules. Only the molecule containing Ni1 will be included in this discussion.

The complex $Ni^{II}H_2pmb(Cl)_2$ is five-coordinate with a coordination geometry that is best described as distorted trigonal bipyramidal (Fig. 2A). The nickel center is positioned nearly within (0.007 Å) the trigonal plane defined by the chloro ligands and the apical nitrogen atom N1. The H_2pmb ligand binds in a meridional manner, with N1 and pyridyl nitrogen (N2, N3) atoms coordinated to the nickel center. The Ni–N1 bond distance of 2.031(2) Å is greater than those of the $Ni–N_{py}$ bonds, which have an average bond distance of 2.129(2) Å. The binding of H_2pmb to $Ni^{II}pmb(Cl)_2$ is comparable to that reported for the Ni^{II} complexes of the ligand, *N,N*-bis[(phenylpyridin-2-yl)methyl] benzylamine) (**1**).[xvii] Ligand **1** is similar to H_2pmb, differing only in having appended phenyl groups instead of carboxyamido units. For instance, in the Ni^{II}(**1**)$(CH_3CN)(H_2O)$ complex, **1** also binds meridionally and has similar Ni N bond lengths.

The chloro ligands occupied the remaining coordinate sites with Ni–Cl1 and Ni–Cl2 bond distances of 2.291(1) and 2.269(1) Å. The difference in the Ni–Cl bond length is attributed to the presence of an intramolecular H-bonding network that surrounds Cl1. Two intramolecular H-bonds are present involving Cl1 and NH groups of the appended carboxyamido units. The N4–H and N5–H bonds vectors are directed toward Cl1 producing N···Cl1 distances of 3.211(3) and 3.230(3) Å, which are within the heavy atom distances normally associated with H-bonds.[xix]

Our structural analyses confirmed that treating $Ni^{II}H_2pmb(Cl)_2$ with a base caused deprotonation of one of the carboxyamido groups to form $Ni^{II}Hpmb(Cl)$. A comparison of the molecular structures of these two complexes showed that a large structural change occurs upon deprotonation. $Ni^{II}Hpmb(Cl)$ has a molecular structure that is closer to square pyramidal (Fig. 2B). The N1, N2, and N3 nitrogen atoms of $[Hpmb]^-$ ligand coordinates to the nickel center, similar to what was found in $Ni^{II}H_2pmb(Cl)_2$, but in a facial manner. Both the N1–N2 and N1–N3 bond distances of 2.067(3) and 2.006(3) Å are significantly shorter in $Ni^{II}Hpmb(Cl)$ compared to those in $Ni^{II}H_2pmb(Cl)_2$. Moreover, the carboxyamidato oxygen atom O_2 in $Ni^{II}Hpmb(Cl)$ coordinates to the nickel center in $Ni^{II}Hpmb(Cl)$ with a Ni1–O2 bond distance equal to 2.007(3) Å. The final coordination site is filled by the lone chloro ligand that binds at a Ni1–Cl1 bond length of 2.315(1) Å. Unlike in $Ni^{II}H_2pmb(Cl)_2$ the chloro ligand does not form a H-bond—rather, a intramolecular H-bond is formed between the appended carboxyamido groups (the N4···O2 distance is 2.978(3) Å).

3.2.2. Molecular Structures of and $Ni^{II}pmb(THF)$ and $Ni^{II}H_2pmb(\kappa^2\text{-}OAc)(\kappa^1\text{-}OAc)\cdot CH_3CN$—

The complexes $Ni^{II}pmb(THF)$ and $Ni^{II}H_2pmb(\kappa^2\text{-}OAc)(\kappa^1\text{-}OAc)$ crystallized in the triclinic space group $P\bar{1}$ and the monoclinic space group *Pc*, respectively. For $Ni^{II}H_2pmb(\kappa^2\text{-}OAc)(\kappa^1\text{-}OAc)\cdot CH_3CN$, there were two independent, but chemically equivalent, molecules in the asymmetric unit. Only the molecule containing Ni1 will be discussed.

The molecular structure of $Ni^{II}pmb(THF)$ corroborated that deprotonation of both appended carboxyamido groups of H_2pmb caused complete loss of the chloro ligands and coordination of the carbonyl oxygen atoms to the nickel center (Fig. 3A). Facial coordination of the N1, N2, and N3 atoms was observed in Ni^{II}pmb(THF), a binding of the $[pmb]^{2-}$ ligand that is similar to the way $[Hpmb]^-$ binds in Ni^{II}Hpmb(Cl). In Ni^{II}pmb(THF) the carbonyl oxygen atoms O1 and O2 are also coordinated with Ni1–O1 and Ni1–O2 bond distances of 2.011(2) and 2.013(2) Å. Note that unlike in the molecular structures of the Ni^{II}–chloro complexes, Ni^{II}pmb(THF) is six-coordinate, with a THF molecule occupying the final coordination site (Ni1–O3(THF) = 2.175(2) Å).

We have also found that the chloro ligands in $Ni^{II}H_2pmb(Cl)_2$ are removed with Ag^I salts in the presence of acetate ions. The resulting complex, $Ni^{II}H_2pmb(\kappa^2\text{-}OAc)(\kappa^1\text{-}OAc)$ is six-coordinate (Fig. 3B), in which the H_2pmb ligand is bonded to the nickel ion in a meridional manner similar to what was observed in $Ni^{II}H_2pmb(Cl)_2$. The N1–N2 and N1–N3 bond lengths are statistically the same at 2.117(2) and 2.120(2) Å, respectively and the Ni1–N1 bond distance is 2.079(2) Å. The two acetate ions coordinate differently: one is bidentate, having Ni1–O3 and Ni1–O4 bond distances of 2.110(2) and 2.144(2) Å, whereas the other is monodentate, having a Ni1–O5 bond length of 1.999(2) Å. Intramolecular H-bonds were also found in $Ni^{II}H_2pmb(\kappa^2\text{-}OAc)(\kappa^1\text{-}OAc)$ between the acetate ions and the H_2pmb ligand. The heavy atom N4···O5 and N5···O3 distances are approximately at 3.0 Å, which is within the range considered for H-bonds.[xx]

4. Summary

Previous studies have shown the utility of the pyridylcarboxyamido unit in ligand design. We have further demonstrated its usefulness in controlling both the primary and secondary coordination spheres in transition metal complexes. Both $Ni^{II}H_2pmb(Cl)_2$ and $Ni^{II}H_2pmb(\kappa^2\text{-}OAc)(\kappa^1\text{-}OAc)$ have H-bonding networks involving the H_2pmb and bound chloro or acetato ligands. Sequential deprotonation of $Ni^{II}H_2pmb(Cl)_2$ led to the binding of the carboxyamido oxygen atoms with concurrent loss of the chloro ligands. Alteration in the H-bonding networks was also observed upon carboxyamido binding and was completely absent in Ni^{II}pmb(THF). The ability to affect structural changes within both coordination spheres could translate into a method for regulating functional properties, such as substrate binding, in a manner reminiscent of what is found in metalloproteins.

Supplementary Material

Refer to Web version on PubMed Central for supplementary material.

Acknowledgments

We thank the NIH (GM50781) and NSF ((0738252)) for financial support of this work. The NSF funded the purchase of the X-ray instrumentation. We thank M. Takase for help in the molecular structure determinations.

References

i. (a) Lu Y, Valentine JS. Curr Opin Struct Biol. 1997; 7:495–500. [PubMed: 9266170] (b) Natale D, Marque-Rivas JC. Chem Comm. 2008:425–437. [PubMed: 18188459] (c) Marque-Rivas JC. Curr Org Chem. 2007; 11:1434–1449.(d) Steiner T. Angew Chem Int Ed. 2002; 41:48–76.(e) Miller AF. Acc Chem Res. 2008; 41:501–510. [PubMed: 18376853] (f) Jackson TA, Brunold TC. Acc Chem Res. 2004; 37:461–470. [PubMed: 15260508]

ii. Representative examples: Lipscomb WN, Strater N. Chem Rev. 1996; 96:2375–2433. [PubMed: 11848831] Bhaumik D, Medin J, Gathy K, Coleman MS. J Biol Chem. 1993; 268:5464–5470. [PubMed: 8449909] Sideraki V, Mihamedali KA, Wilson DK, Chang Z, Kellems RE, Quiocho FA, Rudolph FB. Biochemistry. 1996; 35:7862–7872. [PubMed: 8672487]

iii. Reviews: Shook RL, Borovik AS. Chem Comm. 2008:6095–6107. [PubMed: 19082087] Borovik AS. Acc Chem Res. 2005; 38:54–61. [PubMed: 15654737] Marque-Rivas JC, Hinchley SL, Metteau L, Parsons S. Dalton Trans. 2006:2316–2322. [PubMed: 16688319]

iv. Harata M, Hasegawa K, Jitsukawa K, Masuda H, Einaga H. Bull Chem Soc, Jpn. 1998; 71:1031–1038.Harata M, Jitsukawa J, Masuda H, Einage H. J Am Chem Soc. 1994; 116:10817–10819.Berreau LM, Mahapatra S, Halfen JA, Young VG Jr, Tolman WB. Inorg, Chem. 1996; 35:6339–6342.

v. Mareque-Rivas JC, Salvagni E, Parsons S. Dalton Trans. 2004:4185–4192. [PubMed: 15573171] Natale D, Mareque-Rivas JC. Chem Commun. 2008:425–437.Mareques Rivas JC, de Rosales RTM, Parsons S. Dalton Trans. 2003:2156–2163.Mareques Rivas JC, Salvagni E, de Rosales RTM, Parsons S. Dalton Trans. 2003:3339–3349.(e)

vi. (a) Ingle GK, Makowska-Grzyka MM, Arif AM, Berreau LM. Eur J Inorg Chem. 2007:5262–5269. (c) Rudzka K, Arif AM, Berreau LM. J Am Chem Soc. 2006; 128:17018–17023. [PubMed: 17177453] (c) Berreau LM, Makowska-Grzyska MM, Arif AM. Inorg Chem. 2000; 39:4390–4391.(d) Szajna E, Makowska-Grzyska MM, Wasden CC, Arif AM, Berreau LM. Inorg Chem. 2005; 44:7595–7605. [PubMed: 16212386] (e) Rudzka K, Arif AM, Berreau LM. Inorg Chem. 2005; 44:7234–7242. [PubMed: 16180888] (f) Ingle GK, Makowska-Grzyska MM, Szajna-Fuller E, Sen I, Price JC, Arif AM, Berreau LM. Inorg Chem. 2007; 46:1471–1480. [PubMed: 17249660] (g) Grubel K, Fuller AL, Chambers BM, Arif AM, Berreau LM. Inorg Chem. 2010; 49:1071–1081. [PubMed: 20039645]

vii. Shook RL, Gunderson WA, Greaves J, Ziller JW, Hendrich MP, Borovik AS. J Am Chem Soc. 2009; 130:8888–8889. [PubMed: 18570414]

viii. Shook RL, Borovik AS. Inorg Chem. 2010; 49:0000.

ix. (a) Evans DF. J Chem Soc. 1959:2003.(b) Ostfeld D, Cohen IA. J Chem Educ. 1972; 49:829.

x. Data Collection: SMART Software Reference Manual. Bruker-AXS; Madison, WI: 1994.

xi. Data Reduction: SAINT Software Reference Manual. Bruker-AXS; Madison, WI: 1995.

xii. Sheldrick, GM. SADABS, Version 2.10. Bruker Analytical X-Ray Systems, Inc; Madison, WI: 2002.

xiii. Sheldrick, GM. SHELXTL Version 6.12. BrukerAnalytical X-Ray Systems, Inc; Masdison, WI: 2001.

xiv. International Tables for X-ray Crystallography. Vol. C. Dordrecht: Kluwer Academic Publishers; 1992.

xv. Speck, AL. PLATON, a multipurpose crystallographic tool. Utrecht University; Utrecht, The Netherlands: 2001.

xvi. Sheldrick, GM. SADABS, Version 2008/1. Bruker AXS, Inc; Madison, WO: 2008.

xvii. Kunishita A, Doi Y, Kubo M, Ogura T, Sugimoto H, Itoh S. Inorg Chem. 2009; 48:4997–5004. [PubMed: 19374371]

xviii. Drago, R. Physical Methods in Inorganic Chemistry. Vol. chapter 11. Saunders; Philadelphia: 1977.

xix. (a) Steiner T. Acta Crystallogr, Sec B. 1998; 54:456–463.(b) Aullón G, Bellamy D, Brammer L, Bruton EA, Orpen AG. Chem Commun. 1998:653–654.

xx. (a) Jeffrey, GA. An Introduction to Hydrogen Bonding. Oxford University Press, Inc; New York: 1997. (b) Desiraju, GR.; Steiner, T. The Weak Hydrogen Bond in Structural Chemistry and Biology. Oxford University Press Inc; New York: 1999.

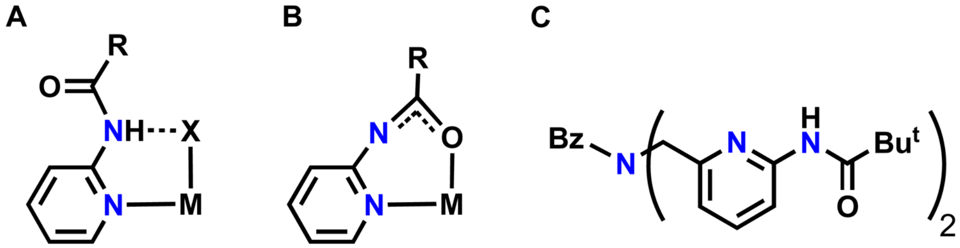

Fig. 1.

The carboxyamido unit used to form an intramolecular H-bond (**A**), to form a bidentate ligand (**B**), and the H_2pmb ligand used in this study (**C**).

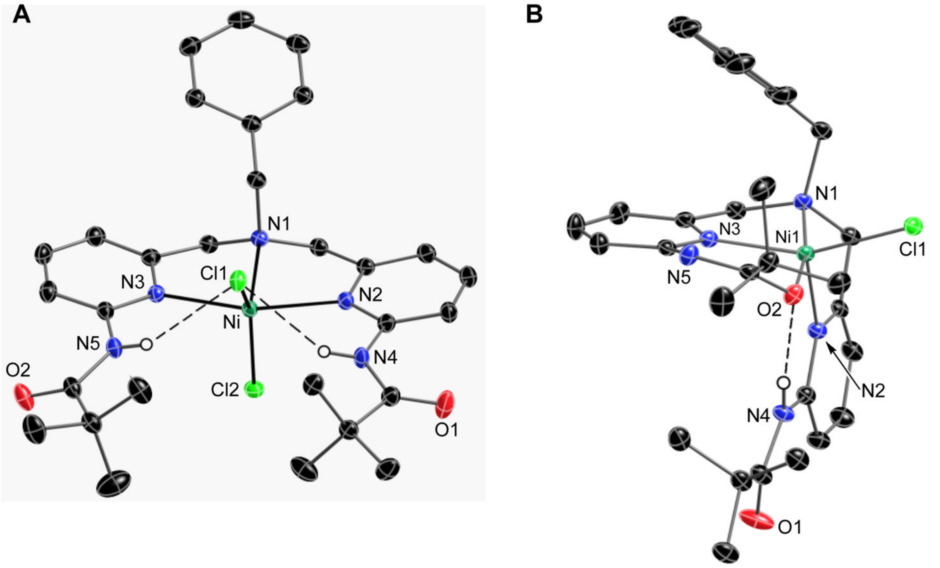

Fig. 2.

Thermal ellipsoid diagrams of $Ni^{II}H_2$ pmb(Cl_2) (**A**) and Ni^{II}Hpmb(Cl) (**B**). The ellipsoids are drawn at the 50% probability level and all non-carboxyamido hydrogen atoms are removed for clarity.

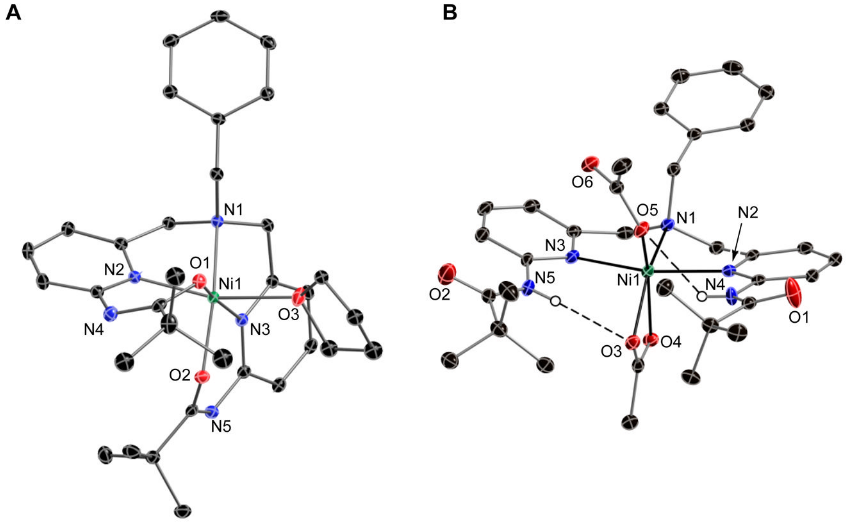

Fig. 3.

Thermal ellipsoid diagrams Ni^{II}pmb(THF) (**A**) and $Ni^{II}H_2$ pmb(κ^2-OAc)(κ^1-OAc) (**B**). The ellipsoids are drawn at the 50% probability level and all non-carboxyamido hydrogen atoms are removed for clarity.

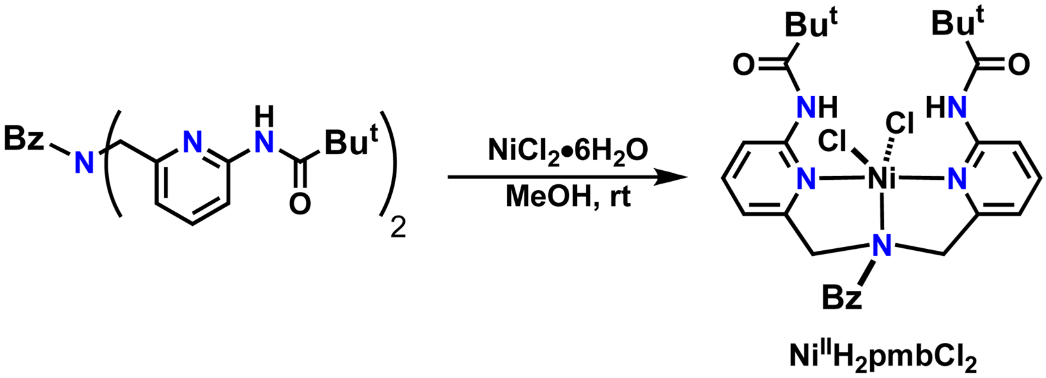

Scheme 1.

Preparative route to $Ni^{II}H_2pmb(Cl)_2$.

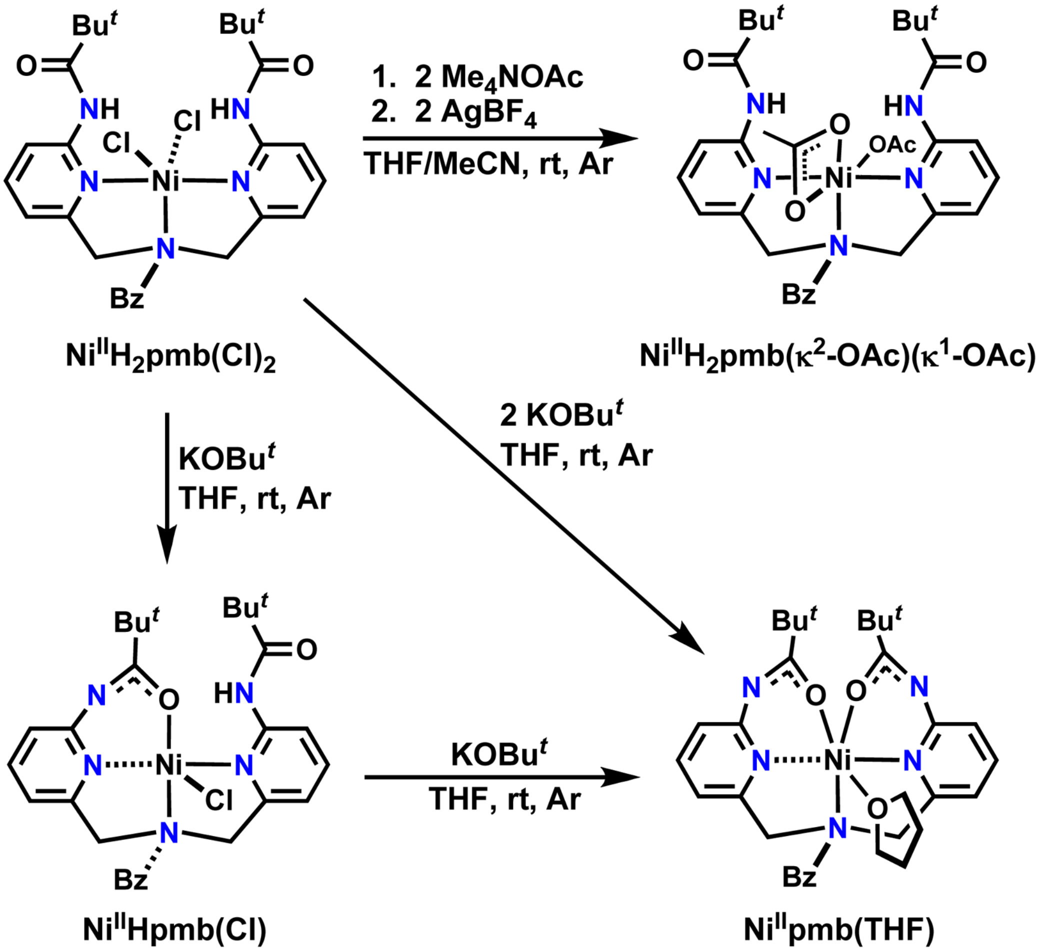

Scheme 2.

Preparative routes to Ni^{II}Hpmb(Cl), Ni^{II}pmb(THF), and Ni^{II}H$_2$pmb(κ^2-OAc)(κ^1-OAc).

Table 1

Crystallographic data for $Ni^{II}H_2pmb(Cl)_2$, $Ni^{II}Hpmb(Cl)$, $Ni^{II}pmb(THF)$, and $Ni^{II}H_2pmb(\kappa^2\text{-}OAc)(\kappa^1\text{-}OAc)\cdot CH_3CN$.

Complex	$Ni^{II}H_2pmb(Cl)_2$	$Ni^{II}Hpmb(Cl)$	$Ni^{II}pmb(THF)$	$Ni^{II}H_2pmb(\kappa^2\text{-}OAc)(\kappa^1\text{- }OAc)_2\cdot CH_3CN$
molecular formula	$C_{29}H_{37}NiN_5O_2Cl_2$	$C_{29}H_{36}NiN_5O_2Cl$	$C_{33}H_{43}NiN_5O_3$	$C_{35}H_{46}NiN_6O_6$
formula weight	617.25	580.79	616.43	705.49
T (K)	153(2)	148(2)	98(2)	153(2)
space group	$P2_1/c$	$P2_1/n$	$P\bar{1}$	Pc
a (Å)	9.3786(5)	17.9869(18)	9.8123(5)	13.452(2)
b (Å)	18.1064(9)	11.6153(12)	11.8641(6)	14.834(3)
c (Å)	17.4684(9)	28.718(3)	13.4619(7)	17.896(3)
α (deg)	90	90	82.8894(7)	90
β (deg)	93.4637(6)	102.5698(14)	82.2732(7)	102.073(2)
γ (deg)	90	90	88.6757(7)	90
Z	4	8	2	4
V (Å^3)	2960.9(3)	5856.0(10)	1540.95(14)	3492.4(10)
δ_{calc} (Mg/m^3)	1.385	1.318	1.329	1.342
R^a	0.0382	0.0627	0.0399	0.0363
$R_w{}^b$	0.1028	0.1494	0.0969	0.0735
GOF^c	1.053	1.098	1.028	1.004
Largest diff. peak (eÅ^3)	1.803	1.450	1.011	0.447

[a] $R = [\Sigma|\Delta F|/\Sigma|F_O|]$.

[b] $R_W = [\Sigma\omega(\Delta F)^2/\Sigma\omega F_O{}^2]$.

[c] goodness of fit on F^2.

Table 2

Selected bond distances and angles for $Ni^{II}H_2pmb(Cl)_2$ and $Ni^{II}Hpmb(Cl)$.

Complex	$Ni^{II}H_2$ pmbCl_2	Ni^{II}HpmbCl
	Distances (Å)	
Ni1—N1	2.031(2)	2.081(3)
Ni—N2	2.125(2)	2.067(3)
Ni—N3	2.134(2)	2.006(3)
Ni—Cl1	2.291(1)	2.315(1)
Ni—Cl2	2.269(1)	–
Ni—O2	–	2.007(3)
Cl1···N4	3.211(6)	–
Cl1···N5	3.230(6)	–
O2···N4	–	2.978(1)
	Angles (deg)	
N1—Ni1—N2	81.64(7)	80.71(13)
N1—Ni1—N3	81.69(7)	82.89(13)
N2—Ni1—N3	163.24(7)	102.26(13)
N1—Ni1—Cl1	114.31(5)	94.24(9)
N1—Ni1—Cl2	101.50(5)	–
N2—Ni1—Cl1	92.81(5)	101.76(9)
N2—Ni1—Cl2	92.82(5)	–
N3—Ni1—Cl1	92.44(5)	155.00(10)
N3—Ni1—Cl2	92.20(5)	–
Cl1—Ni1—Cl2		–
N1—Ni1—O2	–	169.56(12)
N2—Ni1—O2	–	105.94(12)
N3—Ni1—O2	–	87.76(12)
Cl1—Ni1—O2	–	92.27(8)

Table 3

Selected bond distances and angles for Ni^{II}pmb(THF) and $Ni^{II}H_2$pmb(κ^2-OAc)(κ^1-OAc)·CH_3CN.

Complex	Ni^{II}pmb(THF)	$Ni^{II}H_2$pmb (κ^2 -OAc) (κ^1-OAc))·CH_3CN
	Distances (Å)	
Ni—N1	2.166(2)	2.079(2)
Ni—N2	2.022(2)	2.117(2)
Ni—N3	2.052(2)	2.120(2)
Ni—O1	2.001(2)	–
Ni—O2	2.013(2)	–
Ni—O3	–	2.110(2)
Ni—O4	–	2.144(2)
Ni—O5	–	1.999(2)
Ni—O3(THF)	2.175(2)	–
O3···N5	–	3.063(8)
O5···N4	–	3.000(8)
	Angles (deg)	
N1—Ni—N2	77.72(7)	80.49(9)
N1—Ni—N3	77.09(7)	82.59(9)
N2—Ni—N3	109.08(7)	163.07(8)
N1—Ni—O1	107.91(6)	–
N2—Ni—O1	81.83(7)	–
N3—Ni—O1	168.93(6)	–
O1—Ni—O2	89.72(6)	–
O2—Ni—N2	97.14(6)	–
O2—Ni—N3	87.08(6)	–
N1—Ni—O3	–	154.16(8)
N1—Ni—O4	–	92.09(8)
N1—Ni—O5	–	110.99(8)
N2—Ni—O3	–	98.27(8)
N2—Ni—O4	–	91.54(8)
N2—Ni—O5	–	89.70(8)
N3—Ni—O3	–	97.21(8)
N3—Ni—O4	–	89.67(8)
N3—Ni—O5	–	95.81(8)
O3—Ni—O4	–	62.08(7)
O3—Ni—O5	–	94.78(8)
O4—Ni—O5	–	156.75(8)